

Diversion of Electron Flow from Methanogenesis to Crystalline Fe(III) Oxide Reduction in Carbon-Limited Cultures of Wetland Sediment Microorganisms

Eric E. Roden*

Department of Biological Sciences, The University of Alabama, Tuscaloosa, Alabama 35487-0206

Received 17 January 2003/Accepted 26 May 2003

Electron flow in acetate-limited cultures of wetland sediment microorganisms was diverted from methane production to Fe(III) reduction in the presence of crystalline Fe(III) oxides at surface area loadings equivalent to that of amorphous Fe(III) oxide. The results indicate that inferences regarding the ability of microbial Fe(III) oxide reduction to compete with other terminal electron-accepting processes in anoxic soils and sediments should be based on estimates of bulk microbially available surface site abundance rather than assumed thermodynamic properties of the dominant oxide phase(s) in the soil or sediment.

Amorphous Fe(III) oxides are generally considered to be the main form of Fe(III) oxide available for dissimilatory microbial reduction in hydromorphic soils and sediments (9). Sulfate reduction and methane production are inhibited in environments containing abundant amorphous Fe(III) oxides as a result of the competition of Fe(III)-respiring microorganisms (FRM) with sulfate-reducing and methanogenic microorganisms (MGM) for fermentation intermediates such as acetate and H₂ (1, 11, 12, 18) and/or utilization of Fe(III) oxides as alternative electron sinks by sulfate reducers (3, 13) and MGM (2). Recent studies indicate that natural crystalline Fe(III) oxides (e.g., goethite and hematite) are subject to considerable enzymatic reduction by FRM; in many cases their percentages of reduction are severalfold higher than those of their synthetic counterparts (20, 26). In addition, significant reductions in crystalline Fe(III) oxide phases have been documented for landfill leachate- (6) and petroleum hydrocarbon (25)-contaminated aquifer sediments, as well as for pristine coastal plain aquifer sediments amended with electron donors and inorganic nutrients (17).

Studies of the kinetics of microbial synthetic Fe(III) oxide reduction indicate that initial rates of reduction are directly correlated with oxide surface area, such that surface area-normalized reduction rates are comparable across a wide range of oxide minerals with various crystal structures and levels of stability (16, 20). These findings suggest that FRM may divert electron flow away from other terminal-electron-accepting processes (TEAPs) in anoxic soils and sediments using crystalline Fe(III) oxides as electron acceptors, if the crystalline Fe(III) oxides are present at bulk surface area loadings comparable to those typical for amorphous Fe(III) oxides in sedimentary environments. A survey of published data on amorphous Fe(III) oxide abundance in hydromorphic soils, aquatic sediments, and subsurface sediments (available from the author upon request) yielded a range of concentrations of ca. 1 to

100 mmol per liter of wet sediment, which corresponds to volumetric surface area loadings of 53 to 2,670 m² liter⁻¹, assuming standard values of 89 g mol⁻¹ and 600 m² g⁻¹ for the gram molecular weight and specific surface area of amorphous hydrous ferric oxide, respectively (5).

In this study, the potential for FRM to compete effectively with MGM with crystalline Fe(III) oxides as electron acceptors was examined in organic carbon-limited enrichment cultures of wetland sediment microorganisms. The sediment inoculum for the experiments was obtained from a freshwater wetland located in the Talladega National Forest in north central Alabama. Previous studies have shown that microbial Fe(III) oxide reduction mediates significant organic carbon metabolism and suppresses methanogenesis in Fe(III) oxide-rich surface sediments in the wetland (19) and that FRM compete effectively with MGM for acetate metabolism in surface sediments (18). Most-probable-number enumerations revealed comparable numbers (ca. 10⁷ cells ml⁻¹) of acetate-utilizing FRM and MGM in the surface sediment inoculum.

A preliminary experiment demonstrated that the presence of 10 mmol of freshly precipitated amorphous hydrous ferric oxide (HFO) liter⁻¹ led to substantial Fe(II) production (determined via 0.5 M HCl extraction and Ferrozine analysis) and strongly inhibited methane production (determined via gas chromatographic analysis of 100- μ l headspace samples) in acetate-limited (1 mM) PIPES-buffered culture medium [10 mM piperazine-*N,N'*-bis(2-ethanesulfonic acid), dipotassium salt, 0.05 mM KH₂PO₄, and 0.5 mM NH₄Cl equilibrated with 100% N₂; initial pH, 6.5 to 6.7] inoculated with a small quantity (1%, vol/vol) of wetland surface sediment (data not shown). In order to examine whether crystalline Fe(III) oxides could cause a similar diversion of electron flow away from methanogenesis, acetate-limited culture medium was amended with synthetic hematite or goethite at concentrations equivalent to the amount of oxide surface area provided by 10 mmol of HFO liter⁻¹ (642 m² liter⁻¹). The hematite (α -Fe₂O₃) powder was purchased from Fisher Scientific, whereas the two goethite (α -FeOOH) phases employed were synthesized in the laboratory (22), either by neutralization of ferric chloride (medium-surface area [MSA] goethite) or slow air oxidation of ferrous

* Mailing address: Department of Biological Sciences, The University of Alabama, A122 Bevell Bldg., 7th Ave., Tuscaloosa, AL 35487-0206. Phone: (205) 348-0556. Fax: (205) 348-1403. E-mail: eroden@bsc.as.ua.edu.

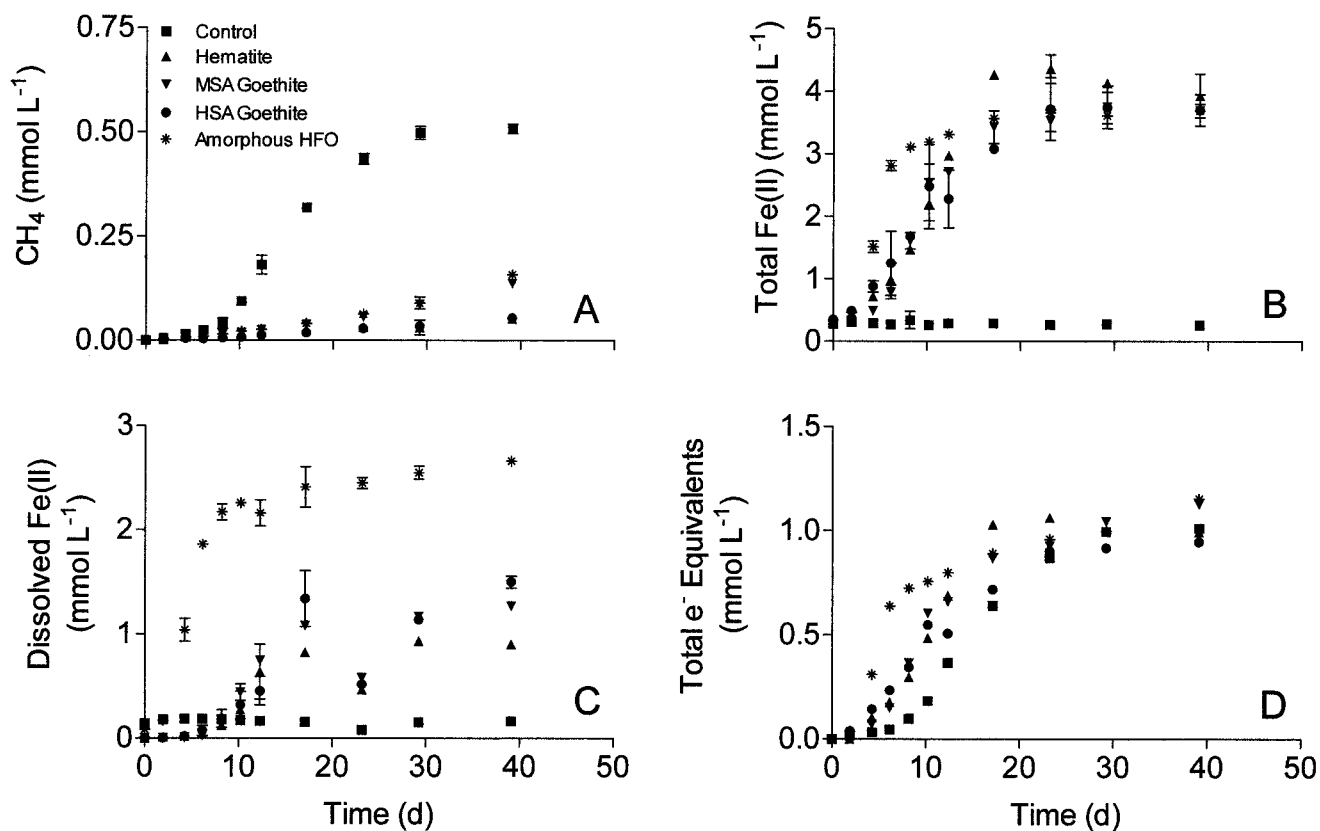


FIG. 1. Methane (A), 0.5 M HCl-extractable Fe(II) (B), and dissolved Fe(II) (C) production in acetate-limited (1 mM) enrichment cultures containing equivalent surface loadings (ca. $640 \text{ m}^2 \text{ liter}^{-1}$) of different Fe(III) oxides (see the text). Control cultures received no Fe(III) oxide addition. Data represent the means \pm ranges of results for duplicate cultures. (D) Total number of electron equivalents metabolized via Fe(III) reduction and/or methane production. d, days.

chloride in bicarbonate buffer (high-surface area [HSA] goethite). Specific surface values for the hematite ($10 \text{ m}^2 \text{ g}^{-1}$) and the two goethite minerals (55 and $210 \text{ m}^2 \text{ g}^{-1}$, respectively) were determined by multipoint Brunauer-Emmett-Teller (BET) N_2 adsorption (Micromeritics; model Gemini). The molar concentrations of Fe(III) added in the forms of hematite, MSA goethite, and HSA goethite were 600, 110, and $28.5 \text{ mmol liter}^{-1}$, respectively. These concentrations are within the range of concentrations of bulk Fe(III) oxide present in natural soils and sediments.

Methane production was as strongly inhibited by the presence of the crystalline Fe(III) oxides as by the presence of amorphous HFO (Fig. 1A). Comparable levels of Fe(II) production occurred in the different Fe(III) oxide-containing cultures (Fig. 1B and C). The total numbers of electron equivalents accounted for by Fe(II) and/or methane accumulation [$0.25 \times \text{Fe(II)} + 2 \times \text{CH}_4$] were comparable among the different treatments (Fig. 1D), which indicates that suppression of methane production was not caused by an inhibitory effect of the Fe(III) oxides on microbial metabolism. The results demonstrate that electron flow was diverted from methane production to Fe(III) reduction in each of the Fe(III) oxide-containing cultures. These findings contrast with those of an earlier study which showed that amorphous Fe(III) oxide, but not crystalline hematite, permitted FRM to dominate MGM in acetate-oxidizing enrichment cultures from freshwater riverine

sediments (12). However, in that study, the concentration (i.e., surface area loading) of hematite [$250 \text{ mmol of Fe(III) liter}^{-1}$, equivalent to ca. $200 \text{ m}^2 \text{ liter}^{-1}$, assuming a hematite surface area of $10 \text{ m}^2 \text{ g}^{-1}$] was likely not sufficient to inhibit methanogenesis in the presence of excess acetate (20 mM).

The influence of Fe(III) oxide surface loading on the ability of FRM to outcompete MGM was explored in acetate-limited (1 mM) cultures containing different amounts of MSA goethite [10 to $100 \text{ mmol of Fe(III) liter}^{-1}$, equivalent to an oxide surface area of ca. 50 to $530 \text{ m}^2 \text{ liter}^{-1}$]. Methanogenesis was only slightly suppressed in cultures containing 10 mmol of Fe(III) liter^{-1} but was progressively suppressed in the presence of increasing amounts of goethite surface (Fig. 2A). The extent of suppression in cultures containing 100 mmol of MSA goethite liter^{-1} ($530 \text{ m}^2 \text{ liter}^{-1}$) was comparable to that observed in a parallel culture amended with 10 mmol of HFO liter^{-1} ($640 \text{ m}^2 \text{ liter}^{-1}$) (Fig. 2A, inset). The amount of Fe(II) produced was linearly correlated with oxide surface loading (Fig. 2B and C), whereas the amount of CH_4 produced decreased logarithmically (Fig. 2C). The results of this experiment indicated that FRM were able to compete effectively with MGM when the initial ratio of Fe(III) oxide surface area to acetate concentration was greater than ca. $125 \text{ m}^2 \text{ mmol}^{-1}$ [initial concentration of MSA goethite, $\geq 25 \text{ mmol of Fe(III) liter}^{-1}$], a value ca. 10-fold greater than that present in the hematite-amended enrichment cultures (ca. $10 \text{ m}^2 \text{ mmol}^{-1}$)

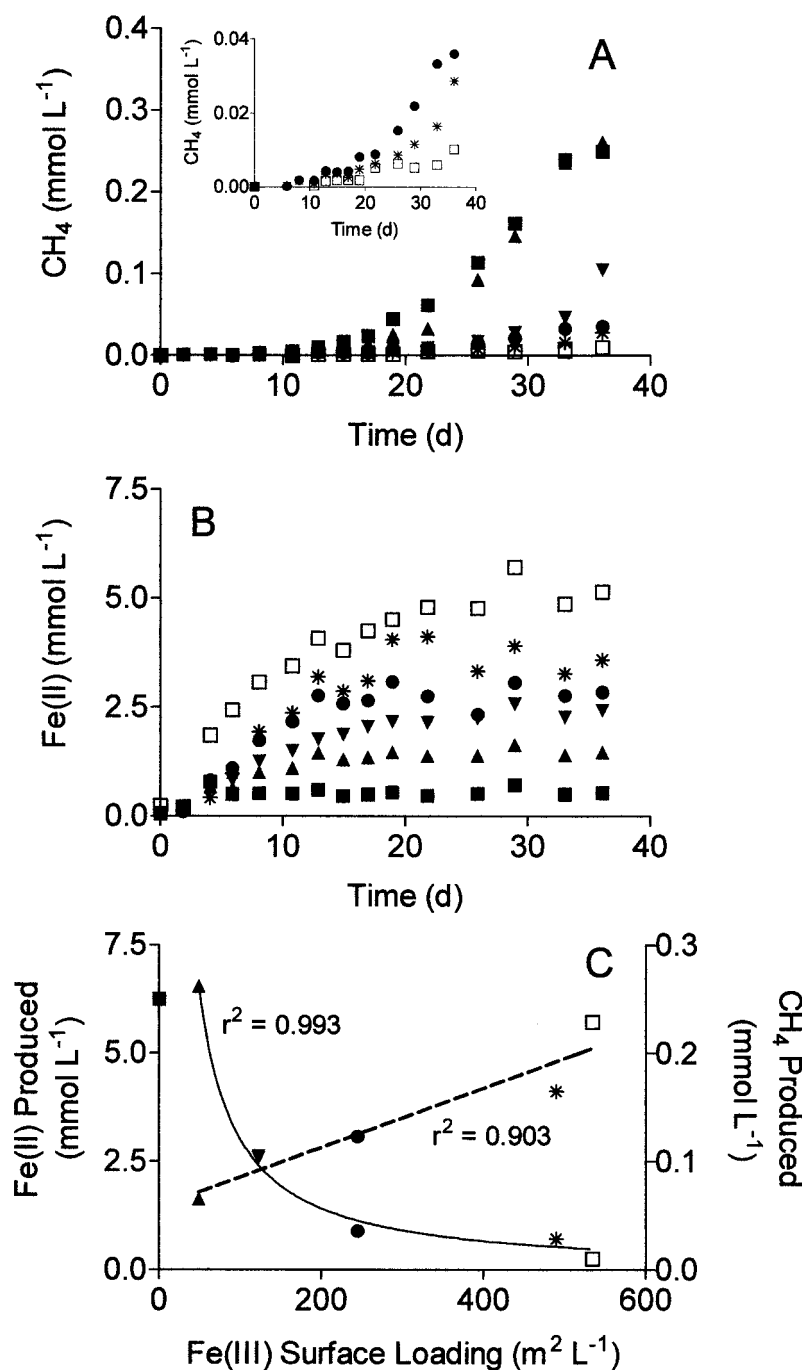


FIG. 2. Methane (A) and 0.5 M HCl-extractable Fe(II) (B) production in acetate-limited (1 mM) enrichment cultures containing 10 (▲), 25 (▼), 50 (●), or 100 (✱) mmol of MSA goethite liter⁻¹ or 10 mmol of amorphous HFO liter⁻¹ (□). Control cultures (■) received no Fe(III) oxide addition. Data represent the means of results from duplicate cultures. The inset in panel A shows data for the 50- and 100-mmol/liter MSA goethite and 10-mmol/liter HFO cultures with an expanded y axis. (C) Maximum amounts of Fe(II) or CH₄ produced in the different cultures as a function of oxide surface loading. The solid line represents a nonlinear least-squares regression fit of the CH₄ production data to a power function ($y = mx^b$; $m = 18.6 \pm 6.1$, $b = -1.09 \pm 0.08$; error terms are standard errors of the regression parameters), and the dashed line represents a linear least-squares regression fit of the data to a straight line ($y = mx + b$; $m = 1.45 \pm 0.45$, $b = 0.00686 \pm 0.00130$; error terms are standard errors of the regression parameters). d, days.

studied by Lovley and Phillips (12). An alternative explanation, relative to that of competitive inhibition, for the suppression of methane production with increasing Fe(III) oxide abundance is that acetoclastic methanogens diverted increasing amounts of reducing equivalents to Fe(III) that would otherwise have

been used to reduce the methyl group of acetate (2). This phenomenon may indeed have been operative in the experiments reported here, since the amount of acetate initially present in the enrichment cultures was ca. 100-fold greater than the estimated K_m for acetate uptake by methanogens in

TABLE 1. Stoichiometric reactions, initial reactant and product concentrations, and initial ΔG values for acetate oxidation coupled to acetoclastic methanogenesis and to the reduction of different synthetic Fe(III) oxide phases

Process	Reaction	Initial ΔG (kJ rxn ⁻¹) ^a
Acetoclastic methanogenesis	$\text{CH}_3\text{COO}^- + \text{H}_2\text{O} \rightarrow \text{CH}_4 + \text{HCO}_3^-$ (initial $[\text{CH}_3\text{COO}^-] = 1 \text{ mM}$; initial $[\text{CH}_4] = 0.017 \text{ }\mu\text{M}$; initial $[\text{HCO}_3^-] = 0.51 \text{ mM}$)	-60.4
Hematite reduction	$\text{CH}_3\text{COO}^- + 4\text{Fe}_2\text{O}_3 + 15\text{H}^+ \rightarrow 8\text{Fe}^{2+} + 2\text{HCO}_3^- + 8\text{H}_2\text{O}$ (initial $[\text{CH}_3\text{COO}^-] = 1 \text{ mM}$; initial pH = 6.56; initial $[\text{Fe}^{2+}] = 3.7 \text{ }\mu\text{M}$; initial $[\text{HCO}_3^-] = 0.52 \text{ mM}$)	-85.9
MSA goethite reduction	$\text{CH}_3\text{COO}^- + 8\text{FeOOH} + 15\text{H}^+ \rightarrow 8\text{Fe}^{2+} + 2\text{HCO}_3^- + 12\text{H}_2\text{O}$ (initial $[\text{CH}_3\text{COO}^-] = 1 \text{ mM}$; initial pH = 6.69; initial $[\text{Fe}^{2+}] = 1.8 \text{ }\mu\text{M}$; initial $[\text{HCO}_3^-] = 0.68 \text{ mM}$)	-133
HSA goethite reduction	$\text{CH}_3\text{COO}^- + 8\text{FeOOH} + 15\text{H}^+ \rightarrow 8\text{Fe}^{2+} + 2\text{HCO}_3^- + 12\text{H}_2\text{O}$ (initial $[\text{CH}_3\text{COO}^-] = 1 \text{ mM}$; initial pH = 6.64; initial $[\text{Fe}^{2+}] = 1.5 \text{ }\mu\text{M}$; initial $[\text{HCO}_3^-] = 0.54 \text{ mM}$)	-261
Amorphous HFO reduction	$\text{CH}_3\text{COO}^- + 8\text{Fe}(\text{OH})_3 + 15\text{H}^+ \rightarrow 8\text{Fe}^{2+} + 2\text{HCO}_3^- + 20\text{H}_2\text{O}$ (initial $[\text{CH}_3\text{COO}^-] = 1 \text{ mM}$; initial pH = 6.64; initial $[\text{Fe}^{2+}] = 86.0 \text{ }\mu\text{M}$; initial $[\text{HCO}_3^-] = 0.61 \text{ mM}$)	-765

^a Oxide ΔG_f values (in kilojoules per mole): for hematite, -740; for MSA goethite, -483; for HSA goethite, -468; and for amorphous HFO, -632.

Talladega Wetland (18) and other freshwater sediments (10). However, regardless of the mechanism(s) involved, the important point is that a nearly quantitative diversion of the electron flow from methanogenesis to Fe(III) reduction was possible when crystalline Fe(III) oxides were present at surface loadings equivalent to that of amorphous HFO.

In order to assess potential thermodynamic controls on competition between FRM and MGM for acetate, the free energy associated with acetate oxidation coupled to the reduction of the different Fe(III) oxides or to acetoclastic methanogenesis (data from Fig. 1; see Table 1 for details) was computed based on measured values of dissolved Fe(II) (Ferrozine analysis of culture samples with a 0.2- μm -pore-size filter), the pH (Orion combination electrode), and amounts of dissolved inorganic carbon and methane (gas chromatographic analysis of pCO_2 and pCH_4 in the culture bottle headspace) converted to aqueous-phase concentrations using Henry's Law constants (listed in reference 23). An initial acetate concentration of 1 mM was assumed for the calculations, and changes in acetate concentration (not measured) were computed based on the number of electron equivalents accounted for by Fe(II) and/or methane accumulation. Activity coefficients for charged ions (Fe^{2+} , HCO_3^- , and CH_3COO^-) were computed using the Davies equation (23), assuming an ionic strength of 0.02 M based on the concentrations of the major ions present in the culture medium. Free energies of formation (ΔG_f values) for the different oxides were estimated from standard values (4) and particle size- ΔG_f relationships (24) as described elsewhere (16).

The results of the ΔG calculations indicated major differences in the initial free energy of acetate oxidation coupled to the reduction of the different Fe(III) oxide phases (Table 1). In the case of hematite reduction, the initial ΔG value was only slightly (ca. 25 kJ reaction $[\text{rxn}]^{-1}$) higher than that for methanogenesis. Increases in pH (from pH 6.6 to 6.7 to pH 6.8 to 7.0) and dissolved Fe(II) (from 1.8 to 86 μM to 0.90 to 2.7 mM) (Fig. 1C) during Fe(III) oxide reduction led to significant shifts (to more positive values) in computed ΔG values for the reduction of all of the oxides (Fig. 3). In the cases of hematite and MSA goethite reduction, ΔG values became more positive than those estimated for methanogenesis after only a few days of incubation. Nevertheless, diversion of electron flow from methanogenesis to Fe(III) reduction was evident for ca. 2 weeks in these cultures (Fig. 1A and B). Moreover, estimated ΔG values for hematite and MSA goethite reduction

became more positive than the theoretical minimum value of ca. -20 kJ rxn⁻¹ required to exploit the free energy change in a reaction (21) at a time (ca. 10 days) when active Fe(III) oxide reduction was still occurring. Comparable results were obtained from calculations performed on the data shown in Fig. 2. Together these observations cast doubt on the ability of thermodynamic calculations employing standard Fe(III) oxide ΔG_f values (e.g., references 7, 8, and 15) to provide accurate insight into the capacity of microbial Fe(III) oxide reduction to compete as a TEAP in anoxic soils and sediments. Diversion of electron flow from methanogenesis to crystalline Fe(III) oxide reduction was clearly possible despite the fact that the theoretical thermodynamic substantially favored amorphous over crystalline Fe(III) oxide reduction. Accurate assessment of the energetics of solid-phase Fe(III) oxide reduction will require more-detailed information on the thermodynamic properties of the oxide surface phases actually undergoing enzymatic reduction, as well as those of the Fe(III) reductase systems responsible for electron transfer (17), including the hydrogenase systems of acetoclastic methanogens that are presumably capable of transferring electrons to Fe(III) (2).

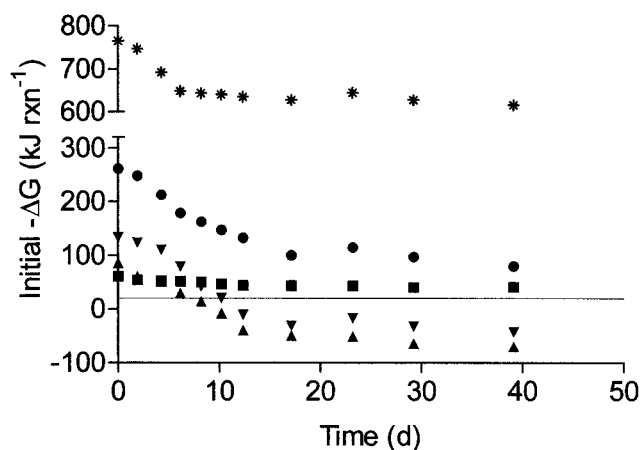


FIG. 3. Computed ΔG values for acetate oxidation coupled to Fe(III) oxide reduction or acetoclastic methanogenesis (control). Symbols are as defined in the legend to Fig. 1. Data represent calculations based on means of the results for duplicate cultures depicted in Fig. 1. See the text and Table 1 for descriptions of the calculations. The horizontal line represents the theoretical minimum energy required for ATP biosynthesis (-20 kJ rxn⁻¹ [21]). d, days.

The findings described above are consistent with the recent demonstration (using a pure FRM culture) that microbial Fe(III) oxide reduction does not respond strongly to oxide thermodynamic properties which exert a major impact on the kinetics of abiotic reductive dissolution (16). Available evidence suggests that FRM transfer electrons to various Fe(III) oxide surfaces with nearly equal efficiencies, regardless of the crystal structure of the underlying oxide mineral. This phenomenon is clearly illustrated by the results of the present study: rates of Fe(II) accumulation were comparable for the different oxides when they were present at equal surface loadings (Fig. 1B). These findings indicate that inferences regarding the ability of microbial Fe(III) oxide reduction to suppress other TEAPs in anoxic soils and sediments should be based on estimates of bulk reactive (i.e., microbially accessible) surface site abundance rather than assumed thermodynamic properties of the oxide(s) identified as the dominant phase(s) in the soil or sediment. Since crystalline Fe(III) oxides are as reducible, on a surface area basis, as amorphous Fe(III) oxide, less favorable TEAPs are likely to be suppressed as long as the crystalline Fe(III) oxides are sufficiently abundant. It is important to note, however, that accumulation of sorbed and/or surface-precipitated Fe(II) on crystalline Fe(III) oxide surfaces renders those surfaces progressively unreactive toward enzymatic reduction and thereby exerts an important control on the long-term microbial reducibility of crystalline Fe(III) oxides (17). This phenomenon is likely responsible for the preservation of substantial quantities of crystalline Fe(III) oxides in permanently reduced surface and subsurface sediments (e.g., references 14 and 25) and will ultimately govern the degree to which crystalline Fe(III) oxides can serve as competing electron acceptors for organic matter oxidation in a given soil or sedimentary environment.

This research was supported by grant DEB-9407233 from the U.S. National Science Foundation, Ecosystem Studies Program, and grant DE-FG07-96ER62321 from the U.S. Department of Energy, Environmental Management Science Program.

Thanks go to Ken Overstreet for technical assistance.

REFERENCES

- Acht nich, C., F. Bak, and R. Conrad. 1995. Competition for electron donors among nitrate reducers, ferric iron reducers, sulfate reducers, and methanogens in anoxic paddy soil. *Biol. Fertil. Soils* **19**:65–72.
- Bond, D. R., and D. R. Lovley. 2002. Reduction of Fe(III) by methanogens in the presence and absence of extracellular quinones. *Environ. Microbiol.* **4**:115–124.
- Coleman, M. L., D. B. Hedrick, D. R. Lovley, D. C. White, and K. Pye. 1993. Reduction of Fe(III) in sediments by sulphate-reducing bacteria. *Nature* **361**:436–438.
- Cornell, R. M., and U. Schwertmann. 1996. The iron oxides. VCH, New York, N.Y.
- Dzombak, D. A., and F. M. M. Morel. 1990. Surface complexation modeling: hydrous ferric oxide. John Wiley & Sons, New York, N.Y.
- Heron, G., and T. H. Christensen. 1995. Impact of sediment-bound iron on redox buffering in a landfill leachate polluted aquifer (Vejen, Denmark). *Environ. Sci. Technol.* **29**:187–192.
- Jakobsen, R., H. J. Albrechtsen, M. Rasmussen, H. Bay, P. Bjerg, and T. H. Christensen. 1998. H₂ concentrations in a landfill leachate plume (Grindsted, Denmark): *in situ* energetics of terminal electron acceptor processes. *Environ. Sci. Technol.* **32**:2142–2148.
- Jakobsen, R., and D. Postma. 1999. Redox zoning, rates of sulfate reduction and interactions with Fe-reduction and methanogenesis in a shallow sandy aquifer, Romo, Denmark. *Geochim. Cosmochim. Acta* **63**:137–151.
- Lovley, D. R. 2000. Fe(III) and Mn(IV) reduction, p. 3–30. *In* D. R. Lovley (ed.), *Environmental metal-microbe interactions*. ASM Press, Washington, D.C.
- Lovley, D. R., and M. J. Klug. 1983. Sulfate reducers can outcompete methanogens at freshwater sulfate concentrations. *Appl. Environ. Microbiol.* **45**:187–192.
- Lovley, D. R., and E. J. P. Phillips. 1987. Competitive mechanisms for inhibition of sulfate reduction and methane production in the zone of ferric iron reduction in sediments. *Appl. Environ. Microbiol.* **53**:2636–2641.
- Lovley, D. R., and E. J. P. Phillips. 1986. Organic matter mineralization with reduction of ferric iron in anaerobic sediments. *Appl. Environ. Microbiol.* **51**:683–689.
- Lovley, D. R., E. E. Roden, E. J. P. Phillips, and J. C. Woodward. 1993. Enzymatic iron and uranium reduction by sulfate-reducing bacteria. *Mar. Geol.* **113**:41–53.
- Phillips, E. J. P., D. R. Lovley, and E. E. Roden. 1993. Composition of non-microbially reducible Fe(III) in aquatic sediments. *Appl. Environ. Microbiol.* **59**:2727–2729.
- Postma, D., and R. Jakobsen. 1996. Redox zonation: equilibrium constraints on the Fe(III)/S₀₄-reduction interface. *Geochim. Cosmochim. Acta* **60**:3169–3175.
- Roden, E. E. 2003. Fe(III) oxide reactivity toward biological vs. chemical reduction. *Environ. Sci. Technol.* **37**:1319–1324.
- Roden, E. E., and M. M. Urrutia. 2002. Influence of biogenic Fe(II) on bacterial reduction of crystalline Fe(III) oxides. *Geomicrobiol. J.* **19**:209–251.
- Roden, E. E., and R. G. Wetzel. 2003. Competition between Fe(III)-reducing and methanogenic bacteria for acetate in iron-rich freshwater sediments. *Microb. Ecol.* **45**:252–258.
- Roden, E. E., and R. G. Wetzel. 1996. Organic carbon oxidation and suppression of methane production by microbial Fe(III) oxide reduction in vegetated and unvegetated freshwater wetland sediments. *Limnol. Oceanogr.* **41**:1733–1748.
- Roden, E. E., and J. M. Zachara. 1996. Microbial reduction of crystalline iron(III) oxides: influence of oxide surface area and potential for cell growth. *Environ. Sci. Technol.* **30**:1618–1628.
- Schink, B. 1997. Energetics of syntrophic cooperation in methanogenic degradation. *Microbiol. Mol. Biol. Rev.* **61**:262–280.
- Schwertmann, U., and R. M. Cornell. 1991. Iron oxides in the laboratory. Weinheim, New York, N.Y.
- Stumm, W., and J. J. Morgan. 1996. *Aquatic chemistry*, 2nd ed. John Wiley & Sons, Inc., New York, N.Y.
- Trolard, F., and Y. Tardy. 1987. The stability of gibbsite, boehmite, aluminous goethites and aluminous hematites in bauxites, ferricretes and laterites as a function of water activity, temperature, and particle size. *Geochim. Cosmochim. Acta* **51**:945–947.
- Tuccillo, M. E., I. M. Cozzarelli, and J. S. Herman. 1999. Iron reduction in the sediments of a hydrocarbon-contaminated aquifer. *Appl. Geochem.* **14**:655–667.
- Zachara, J. M., J. K. Fredrickson, S. W. Li, D. W. Kennedy, S. C. Smith, and P. L. Gassman. 1998. Bacterial reduction of crystalline Fe(III) oxides in single phase suspensions and subsurface materials. *Am. Mineral.* **83**:1426–1443.